Chapter 14
Micromechanics of Internal Frictions in Thermoplastic Composites Exposed to High-Frequency Vibrations

Thijs Masmeijer, Ed Habtour, and Dario di Maio

Abstract Recently introduced class of fiber-reinforced thermoplastic polymer composites (FTPC) in aerospace structures offer a high stiffness-to-weight ratio, cost-saving, and recyclability advantages compared to their thermoset composites. However, their structural performance under high-frequency vibratory loads during their service life is not well understood. Such loads instigate internal material friction inside the microcracks. In this paper, we propose a combined dynamic characterization and fracture mechanics modeling for evaluating the evolution of damage precursors (microcracks) in FTPC due to the presence of internal frictional forces. In order to run simulations to calculate self-heating caused by vibration, one must run transient analysis, because of the contact elements which calculate the amount of friction generated. This work proposes for the first time to apply the structure's Operating Deflection Shape as a dynamic load to include that friction. An innovation of the proposed method is the inclusion of microscopic self-heating in the microcracks as a consequence of high-frequency frictional forces. The Finite Element Method (FEM) is utilized to perform the dynamic analysis for a thermoplastic composite beam with a microcrack exposed to high-frequency vibration fatigue.

Keywords Thermoplastic composites · Vibration · Microcracks · Dynamics · Fracture mechanics · Self-heating

14.1 Introduction

Recent advances in sustainable thermoplastic manufacturing have accelerated the development of fiber-reinforced thermoplastic polymer composites (FTPC) structures for aerospace application components. Just like fiber-reinforced thermoset composites, FTPC structures hold promise for aerospace platforms due to their stiffness-to-weight ratio. However, investigations of the damage accumulation in FTPC during operational conditions, such as vibrations, remain underexplored. Studying fatigue in FRPs is essential for understanding the structural integrity of the laminates over their complete service life to ensure the safety of aircraft [1].

Most of the current research related to the structural performance of FTPC is focused on low-loading rate mechanical testing. Mechanical tests mainly consist of tension, or 3- or 4-point bending tests. Fatigue tests span low-cycle fatigue (LCF) to high-cycle fatigue (HCF) and are tested on various stress ratios. It is well known that low mechanical loading rates for fatigue testing can be a labor- and time-intensive process, and often is not reflective of the real-world operational conditions [2]. This makes the alternative to mechanical testing, vibration fatigue testing, a valuable research direction: It has the capability for higher loading rates and often has more representative loading conditions. A challenge of vibration fatigue testing is its susceptibility to self-heating. The increase in the vibration cycles will lead to an increase in the localized self-heating in the adjacent continuum around the microcracks. Subsequently, the thermoplastic polymer matrix will lead to localized material compliance, i.e., localized time-temperature dependence. The effects of higher frequency and temperature require additional tests and the calculation of shift factor(s), as described in [3].

The self-heating effect was observed small quantities of heat generated during the early loading cycles due to visco-elastic conditions and the dissipation of heat in high cycle fatigue [4, 5]. Both these investigations were on quasi-static conditions.

T. Masmeijer (✉) · E. Habtour
The William E. Boeing Department of Aeronautics and Astronautics, University of Washington, Seattle, WA, USA
e-mail: thijsmas@uw.edu; habtour@uw.edu

D. di Maio
Department of Mechanical Engineering, University of Twente, Enschede, Netherlands
e-mail: d.dimaio@utwente.nl

M. Allen et al. (eds.), *Special Topics in Structural Dynamics & Experimental Techniques, Volume 5*,
Conference Proceedings of the Society for Experimental Mechanics Series, https://doi.org/10.1007/978-3-031-37007-6_14

The level of self-heating reported in these studies is much lower than reported in studies on visco-elastic materials [5–12]. The studies all involve mechanical testing at a high enough loading rate to induce self-heating, and all report the detrimental effect of self-heating on the remaining life of composites. One of the major causes for the self-heating is friction at the crack-tip interface during loading [13–15], as shown in Fig. 14.1. One of the limited modeling efforts to estimate the effect of friction in crack growth was performed by Keoschkerjan et al. [16]. This work shows how the self-heating of the material changes the system dynamics. The self-heating effect in composites under vibration has been extensively studied by Katunin et al. [17–31]. These works lead to evaluating fatigue on the self-heating properties; some of those properties were exploited for Structural Health Monitoring. Research is proposed by Shou et al. in [32] about self-heating in a composite particulate under vibration.

The foundation on how to conduct the vibration fatigue test is given by Di Maio et al. [3, 33, 34], Magi et al. [35, 36], and Voudouris et al. [37]. In [36] a modeling approach based on the Virtual Crack Closure Technique (VCCT) is applied to a Finite Element (FE) model undergoing vibration fatigue. The model determines the strain energy release rate at the crack tip as a crack propagates. The strain energy release rate is used as a measure to describe how fast cracks will grow during vibration fatigue tests. In the modeling approach, an automated VCCT routine was written using MatLab, which interacted with FEM solver software ABAQUS. We observe that the routine linking ABAQUS and Matlab is impractical, and obstructs the practical implementation of the approach. In this paper, for the first time, a modeling approach is proposed where building the model and conducting the VCCT analysis was performed within ABAQUS. The VCCT approach was based on calculating the Strain Energy Release Rate at a propagating crack tip. Based on the observation that the self-heating effect is caused by friction at the crack-tip interface [13–15], this work investigates the effect of friction on the VCCT analysis. The all-ABAQUS modeling approach is depicted in Fig. 14.2.

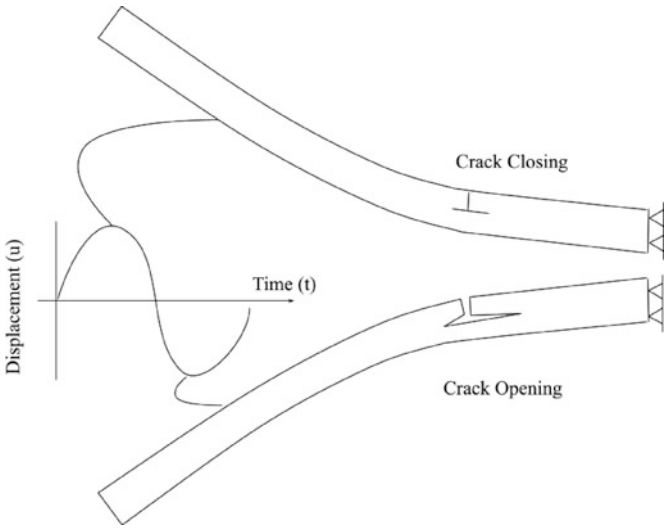

Fig. 14.1 During one oscillation the crack will open and close, causing two different loading conditions

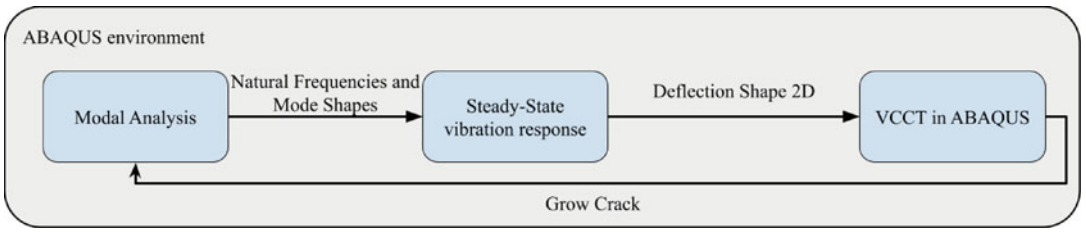

Fig. 14.2 Flowchart diagram of analysis carried out by the FE solvers and outputs similar to [37]. The complete model is run within the ABAQUS environment

14.2 Background

To have predictable and reproducible results, it is common to introduce an artificial transverse crack in the specimen during vibration fatigue tests. The typical failure in composites is due to delimitation, where transverse cracks initiate and grow between the composite laminates. The evolution of the crack is inherently driven by Mixed Mode Conditions, which consist of Mode I: Opening, and Mode II: In-plane Shearing. The vibration load cycle can be described with the closing and opening of a crack, as depicted in Fig. 14.1. During the opening of the crack, Mode I is expected to be dominant, and during the closing of the crack, Mode II is expected to be dominant.

Using VCCT, the energy can be calculated for each mode separately, as expressed by Eq. (14.1) for mode I. The components of Eq. (14.1) are labeled in Fig. 14.3, except for width b of the continuum element and the Strain Energy Release Rate for mode I, G_I. G_{II} is found similarly, but the force and displacement in u-direction are used.

$$G_I = \frac{1}{2}\left(\frac{v_{1,6}F_{v,2,5}}{bd}\right) \tag{14.1}$$

$$G_{II} = \frac{1}{2}\left(\frac{u_{1,6}F_{u,2,5}}{bd}\right) \tag{14.2}$$

Usually an equivalent strain energy release rate (G_{equiv}), and an equivalent critical strain energy release rate ($G_{\text{equiv,C}}$) are calculated for Mixed Mode loading conditions, where $G_{\text{equiv}} = G_I + G_{II}$. $G_{\text{equiv,C}}$ can be found using, for example, the BK-law as described in Benzeggagh [39]. However, we show that this step is not required in this study. The VCCT is developed for quasi-static loading conditions. In quasi-static models, the load (or displacement) is increased incrementally, and cracks are propagated when threshold f is met:

$$f = \frac{G_{\text{equiv}}}{G_{\text{equiv,C}}} \geq 1.0 \tag{14.3}$$

This is not true for fatigue. Under fatigue conditions cracks propagate, despite a low G_{equiv}. In fatigue the crack growth behavior is described using the Paris–Erdogan law:

$$\frac{da}{dN} = C(\Delta K)^m \tag{14.4}$$

where ΔK is the range of the stress intensity factor during a cycle. The crack length is a. The fatigue crack growth for a load cycle N is $\frac{da}{dN}$. C and m are material property constants. Magi [40] proposed that an equivalent law can be set up with ΔK replaced by G_{equiv}, where C and m are updated material constants. The modified Paris-Erodagan law is depicted in Fig. 14.4. The region where the law is representative is marked between the dashed lines.

$$\frac{da}{dN} = C(G_{\text{equiv}})^m \tag{14.5}$$

It is important to point out that since cracks will propagate despite threshold f not being met, the modified modeling approach does not require any values for $G_{\text{equiv,C}}$. This allows us to modify the classic VCCT model, in this paper.

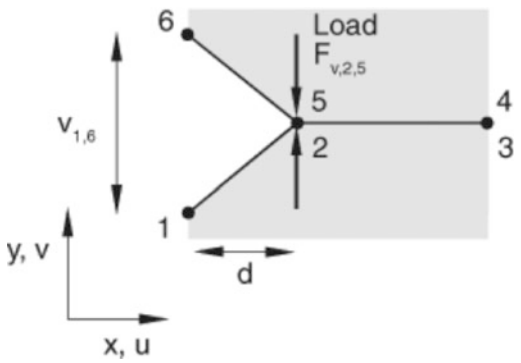

Fig. 14.3 Mode I loading with each component labeled [38]

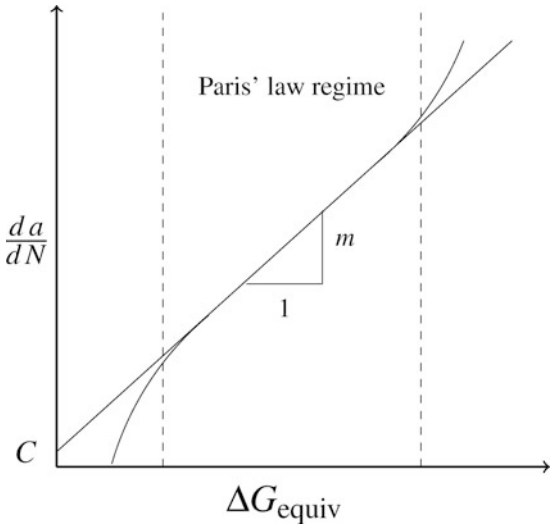

Fig. 14.4 The modified Paris Law by Magi et al. [40] on a log-log scale. The figure is reproduced from [40]

14.3 Analysis

Investigating the change in the Strain Energy Release Rate during the opening of the crack was performed computationally using FEM models in a complete ABAQUS environment. The geometries of each FEM model were replicated from the comparative fracture analyses published by Rarani et al. [41]. In their analysis, they estimated the strain energy release rate for mode I using VCCT, cohesive zone, and XFEM methods and compared them to the experimental results. Their model was utilized to verify a quasi-static VCCT model. Next, the model was modified to represent vibration fatigue tests.

Our proposed model is modified from the quasi-static model to describe vibration fatigue, as depicted in Fig. 14.5. The approach is schematically depicted in Fig. 14.2. Note that every step in this approach is within the ABAQUS environment. The base model was constrained by a single pin at the neutral line on the right side. A 35 mm pre-crack (solid line) was followed by the crack region along the neutral line, shown in the dotted line. The top-left and bottom-left tips of the specimen were assigned a 10 mm displacement upward and downward, respectively.

After verification, the model was modified to investigate the vibration fatigue behavior in thermoplastic composites. The 35 mm pre-crack was removed from the model. The right-side boundary condition was replaced with pins at the top and bottom. This corresponds to a knife edge fixture commonly seen in vibration fatigue tests [33, 35]. A 0.01 mm wide slot was created 15 mm from the right boundary to promote delamination between the plies. The slot depth was the distance from the center line to the beam surface. The slot width was chosen to achieve two objectives: (i) to avoid zero-pivot convergence errors and (ii) to prevent the buckling of the delamination. A crack front will start from the transverse crack towards the pinned boundary. Note, that the slot will promote a crack front that could grow the delamination into or away from the pinned boundary. Tests of similar specimens and materials have shown that delaminations typically grow towards the pinned boundary [42]. The displacement boundary conditions of the top-left and bottom-left tips were removed. During one oscillation in vibration fatigue, the specimen reaches two maximum displacements, as was depicted in Fig. 14.1. A positive displacement corresponded to crack closing and a negative displacement to crack opening. These two absolute orientations were investigated parallel to each other. Each investigation consisted of applying the first vibration mode shape (flexural mode) of the specimen as displacements in, first, the crack opening and, second, the crack closing. The used Operating Deflection Shapes were scaled to always have a fixed displacement at the free tip of 4 mm. To obtain these shapes first eigenvalue extraction was conducted in ABAQUS to obtain the natural frequencies and mode shapes. The step was run with a structural damping coefficient of 0.1%, which was an average of previous run tests on similar materials and was meant to be an indicative value. With the natural frequencies and mode shapes, a mode-based steady-state dynamic analysis step was conducted to obtain the Operating Deflection Shapes. In this step, a -1 N load was applied at the free tip of the specimen. The deflection shapes were acquired separately for each crack length of interest. Finally, the modified VCCT analysis was conducted. Since the critical Strain Energy threshold, f, will never be met, the VCCT step was conducted for each crack length separately. This allowed for matching the deflection shapes to the current crack length.

The used material properties of both models are set out in Table 14.1. The input material properties for the FEM analysis were the longitudinal and transverse elastic moduli (E_1 and E_2, respectively), the shear modulus, G_{12}, and Poisson ratio, ν_{12} [3, 43].

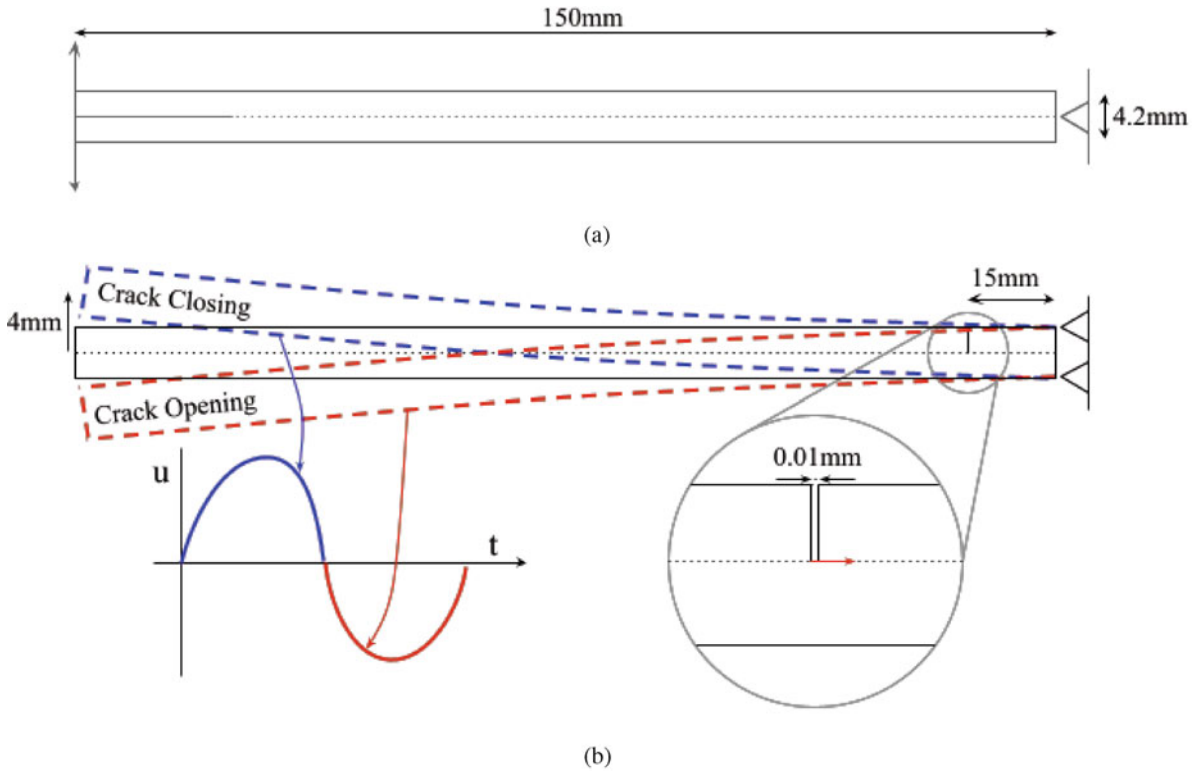

Fig. 14.5 (**a**) Reference model by Rarani et al. [41] used for model verification. (**b**) The modified model for vibration fatigue. (**a**) Base model for verification with Rarani et al. [41]. (**b**) Model for vibration fatigue

Table 14.1 Material properties of the E-glass/epoxy laminate from Rarani et al. [43] used in the reference model. The material properties of PEEK Carbon Fiber were used in previously conducted vibration fatigue tests [3]. The fracture properties for PEEK Carbon Fiber are not necessary since no critical strain energy is required

	E_1 (GPa)	E_2 (GPa)	G_{12} (GPa)	ν_{12}
E-glass/epoxy laminate	33.5	10.23	4.26	0.27
PEEK Carbon Fiber	135	10	5.2	0.28

The FE model included multiple interactions. Two hard contacts were included in the model near the cracked area. The first hard contact was between the two vertical sides of the 0.01 mm wide slot, and the second was between the delamination and the base structure. Tangential behavior was included between the propagating cracks with a fixed friction coefficient (μ) of 0.75, which came from tests conducted by Voudouris et al. [37].

The same mesh and elements (CPE4) were utilized as the 2D VCCT model in Rarani et al. [41]. The thickness of the specimen is divided into 20 elements. The element size was 0.2 mm, which resulted in a total of 15,000 elements. The quasi-static VCCT models were successfully verified with the model from Rarani [41]. The verification results are provided in the appendix.

14.4 Results

Opening the crack causes the Frequency Response Functions (FRFs) to shift, as depicted in Fig. 14.6. An FRF describes the magnitude and phase of the output response as a function of an input frequency. The shift of the FRFs is attributed to a loss of stiffness. Figure 14.7 sets out how the natural frequency drops as the delamination propagates. The drop in natural frequency seems linear with the crack length and the slope is negative. The slope is negative as expected, as the opening of a crack would make the specimen less stiff, i.e., the natural frequency will drop. Remember that a 0.01 mm slot was included between the delamination tips to negate buckling of the delaminations and zero-pivot errors in the Hard contact, as described

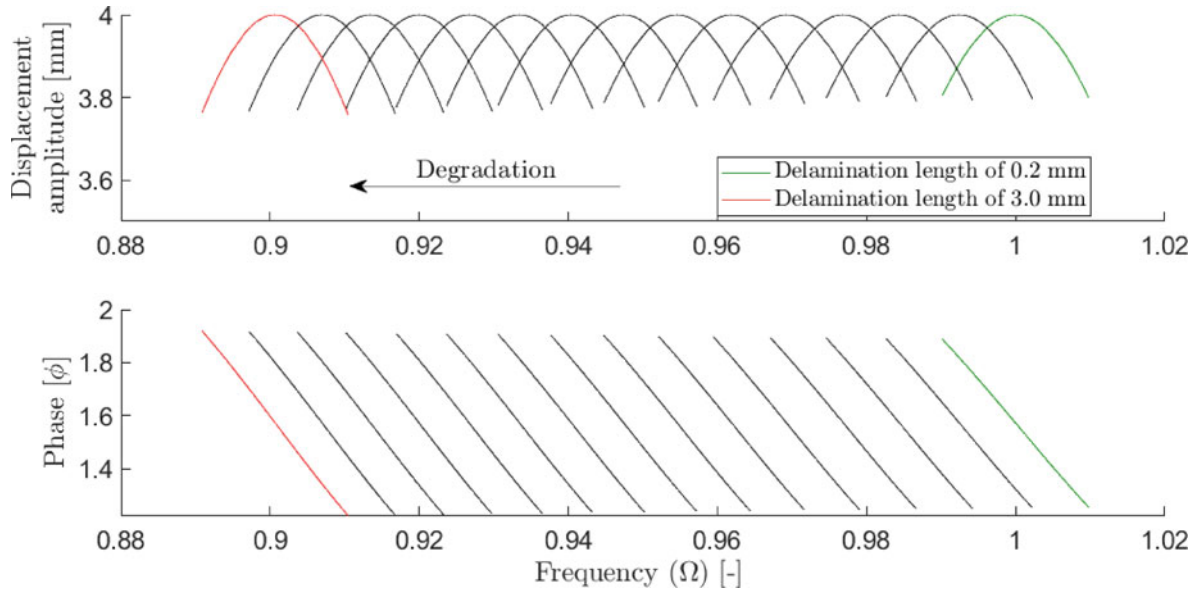

Fig. 14.6 Development of the Frequency Response Function (FRF) due to the growing crack. Note that the FRFs are scaled such that the displacement amplitude at the resonance corresponds to the 4 mm chosen by us. The frequency is normalized according to $\Omega = f/f_{n,1}$, where $f_{n,1}$ is the first natural frequency at the delamination length of 0.2 mm of 204.0 Hz

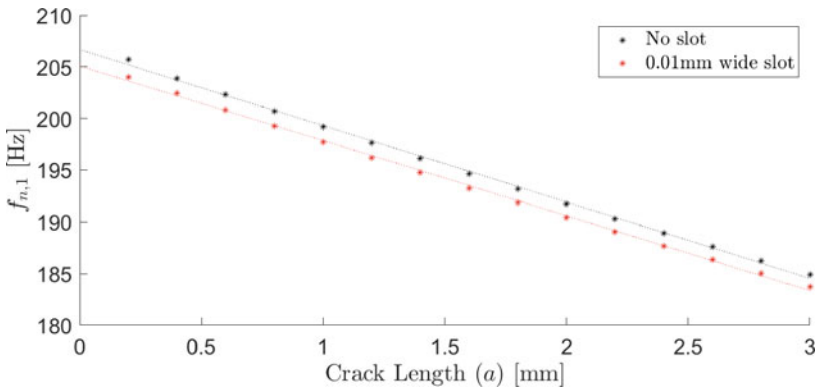

Fig. 14.7 Shift of the natural frequencies due to the propagation of the crack. The intercept and slope of the no-slot model are 206.7 Hz and −7.4 Hz/mm, respectively. The intercept and slope of the model with slot are 205.1 Hz and −7.2 Hz/mm, respectively

in section ANALYSIS. The effect of this slot was a reduction of the natural frequency with −1.6 Hz and had little effect on the slope of the natural frequencies. The reduced natural frequency is as expected because the slot reduces the stiffness of the specimen.

The development of the strain energy release rates for each crack length, ranging from 0.2 mm to 3 mm with steps of 0.2 mm, was set out in Fig. 14.8. Here G_{11} and G_{12} describe mode I (Opening) and mode II (In-plane Shearing), respectively. The results with and without friction are included to compare the effect of friction on the model. The first observation is that the strain energy release rate is significantly higher in the orientation where the crack opens. The difference in G_{ij} between the fiction and no friction case is found to be small compared to the overall G_{ij}. For the crack opening case when the crack is small, we observe that G_{11} is significantly higher than G_{12}. As the crack opens G_{11} first drops quickly and starts to drop linearly at approximately 1 mm. G_{12} first increases and then drops linearly at approximately 1 mm. In the crack closing case when the crack is small G_{11} we observe that Mode II is dominant. As the crack propagates Mode II converges to zero, while Mode I keeps increasing. This is unexpected since when the crack closes, the delamination slides over each other, which is behavior better described by Mode II.

In order to properly compare the effects of friction on crack growth, the differences in G_{ij} were set out in Fig. 14.9. For the crack opening loading condition, the difference in strain energy release rate is zero. This makes sense since the interaction between the delamination and the base structure is inactive when the crack opens. For the crack closing case the difference in G_{12} seems to plateau at 0 as the crack grows. The difference in G_{11} seems to grow as the delamination length increases. We

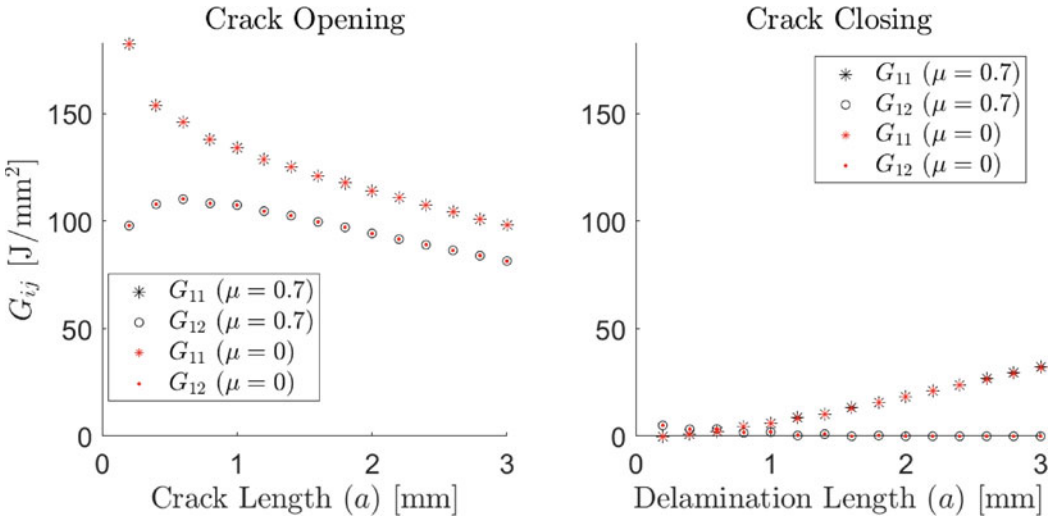

Fig. 14.8 Development of the Strain Energy Release Rate near the fixture (right) with friction ($\mu = 0.7$) and without friction

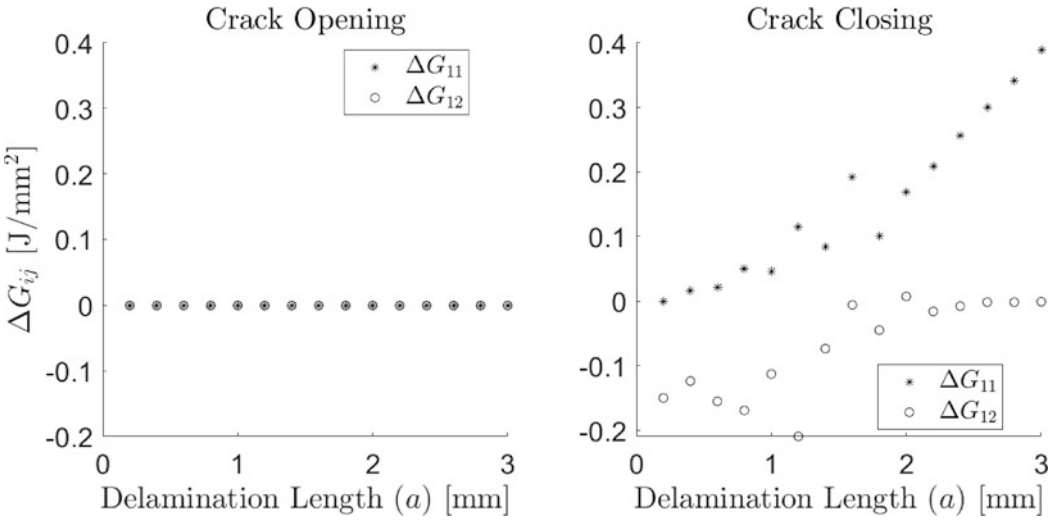

Fig. 14.9 Development of the difference between the Strain Energy Release Rate with friction ($\mu = 0.7$) and without friction. The difference is calculated as the frictionless case minus the case with friction

observe that for the crack closing loading condition some data points have large deviations from the trend. We expect that this behavior comes from the small observed differences caused by the friction component and by instability in the model.

14.5 Conclusion

The modeling approach was able to produce an accurate relationship between the strain energy release rate and the crack length. A previous modeling approach required a link between ABAQUS and Matlab [3]. The novel approach in this work was fully in an ABAQUS environment, removing this major roadblock. The inclusion of friction between the delamination and the base structure had little effect on the absolute results of the strain energy release rate. Nonetheless, the small change in the energy release rate could still be an invaluable indicator for precursors to damage at the micro-scale in fiber-reinforced thermoplastic polymer composites (FTCP). We ask the reader to consider the effects of small deviations in strain energy release rates. In vibration fatigue, where strain energy is released over millions of cycles, the cumulative difference can still have a significant impact on the self-heating behavior of FTPCs. The novel modeling approach allows for further exploration of the behavior of self-heating in fiber-reinforced thermoplastic polymer composites.

Appendix: Verification of the VCCT Model

(Figures 14.10 and 14.11)

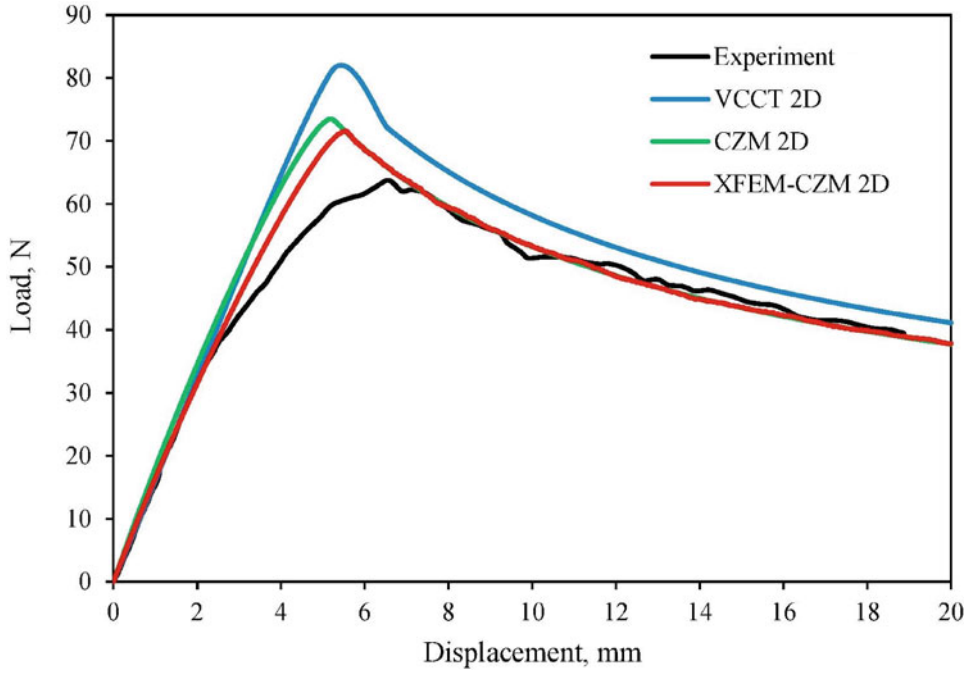

Fig. 14.10 Modelling and experimental results from Rarani et al. [41] and [43]. Figure modified from [41]

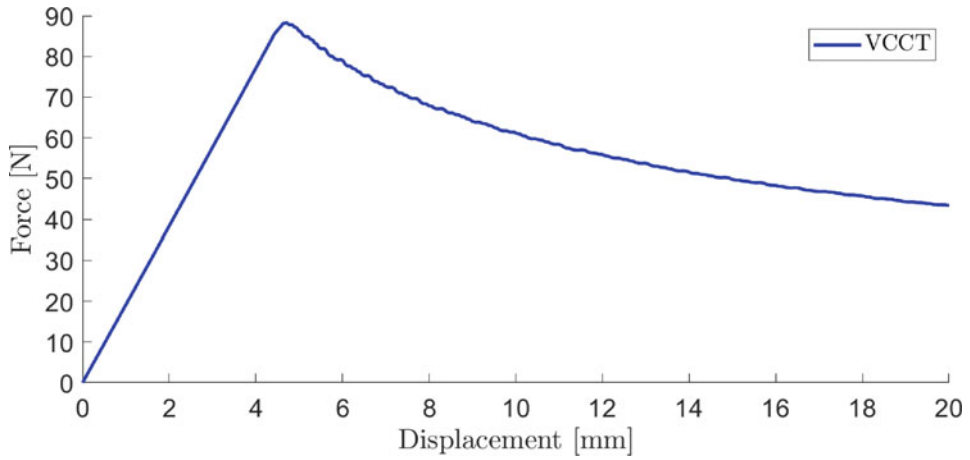

Fig. 14.11 Results from the matched VCCT model

Acknowledgments The authors would like to express their gratitude to the University of Twente and the University of Washington for providing the authors the opportunity to investigate the topics of this paper.

References

1. Alam, P., Mamalis, D., Robert, C., Floreani, C., Ó Brádaigh, C.M.: The fatigue of carbon fibre reinforced plastics—a review. Compos. Part B Eng. **166**, 555–579 (2019)
2. Habtour, E., Di Maio, D., Masmeijer, T., Gonzalez, L.C., Tinga, T.: Highly sensitive nonlinear identification to track early fatigue signs in flexible structures. Journal of Nondestructive Evaluation, Diagnostics and Prognostics of Engineering Systems **5**(2), 021005 (2022)
3. Di Maio, D., Voudouris, G., Sever, I.A.: Investigation of fatigue damage growth and self-heating behaviour of cross-ply laminates using simulation-driven dynamic test. Int. J. Fatigue **155**, 106617 (2022)
4. Maquin, F., Pierron, F.: Heat dissipation measurements in low stress cyclic loading of metallic materials: From internal friction to micro-plasticity. Mech. Mater. **41**, 928–942 (2009)
5. Guo, Q., Zaïri, F., Yang, W.: Evaluation of intrinsic dissipation based on self-heating effect in high-cycle metal fatigue. Int. J. Fatigue **139**, 105653 (2020)
6. Peyrac, C., Jollivet, T., Leray, N., Lefebvre, F., Westphal, O., Gornet, L.: Self-heating method for fatigue limit determination on thermoplastic composites. Procedia Eng. **133**, 129–135 (2015)
7. Shojaei, A.K., Volgers, P.: Fatigue damage assessment of unfilled polymers including self-heating effects. Int. J. Fatigue **100**, 367–376 (2017)
8. Mahmoudi, A., Mohammadi, B.: Theoretical-experimental investigation of temperature evolution in laminated composites due to fatigue loading. Compos. Struct. **225**, 110972 (2019)
9. Pitarresi, G., Scalici, T., Catalanotti, G.: Infrared thermography assisted evaluation of static and fatigue mode II fracture toughness in FRP composites. Compos. Struct. **226**, 111220 (2019)
10. Shen, F., Kang, G., Lam, Y.C., Liu, Y., Zhou, K.: Thermo-elastic-viscoplastic-damage model for self-heating and mechanical behavior of thermoplastic polymers. Int. J. Plast. **121**, 227–243 (2019)
11. Hülsbusch, D., Kohl, A., Striemann, P., Niedermeier, M., Strauch, J., Walther, F.: Development of an energy-based approach for optimized frequency selection for fatigue testing on polymers—exemplified on polyamide 6. Polym. Test. **81**, 106260 (2020)
12. Huang, J., Garnier, C., Pastor, M.L., Gong, X.: Investigation of self-heating and life prediction in CFRP laminates under cyclic shear loading condition based on the infrared thermographic data. Eng. Fract. Mech. **229**, 106971 (2020)
13. Lang, R.W., Manson, J.A.: Crack tip heating in short-fibre composites under fatigue loading conditions. J. Mater. Sci. **22**, 3576–3580 (1987)
14. Huang, J., Li, C., Liu, W.: Investigation of internal friction and fracture fatigue entropy of CFRP laminates with various stacking sequences subjected to fatigue loading. Thin-Walled Struct. **155**, 106978 (2020)
15. Mortazavian, S., Fatemi, A., Mellott, S.R., Khosrovaneh, A.: Effect of cycling frequency and self-heating on fatigue behavior of reinforced and unreinforced thermoplastic polymers. Polym. Eng. Sci. **55**, 2355–2367 (2015)
16. Keoschkerjan, R., Harutyunyan, M., Wurmus, H.: Analysis of self-heating phenomenon of piezoelectric microcomponents actuated harmonically. Microsyst. Technol. **9**, 75–80 (2002)
17. Katunin, A.: Analytical model of the self-heating effect in polymeric laminated rectangular plates during bending harmonic loading. Eksploatacja i Niezawodnosc—Maintenance and Reliability **48**, 91–101 (2010)
18. Katunin, A., Kostka P, H.W., Holeczek, K.: Frequency dependence of the self-heating effect in polymer-based composites. J. Achiev. Mater. Manuf. Eng. **41**(1-2), 9–12 (2010)
19. Katunin, A., Fidali, M.: Experimental identification of non-stationary self-heating characteristics of laminated composite plates under resonant vibration. Kompozyty **11**, 214–219 (2011)
20. Katunin, A.: Critical self-heating temperature during fatigue of polymeric composites under cyclic loading. Compos. Theory Pract. **12**, 72–76 (2012)
21. Katunin, A.: Thermal fatigue of polymeric composites under repeated loading. J. Reinf. Plast. Compos. **31**, 1037–1044 (2012)
22. Katunin, A., Fidali, M.: Fatigue and thermal failure of polymeric composites subjected to cyclic loading. Adv. Compos. Lett. **21**, 096369351202100 (2012)
23. Katunin, A., Fidali, M.: Self-heating of polymeric laminated composite plates under the resonant vibrations: Theoretical and experimental study. Polym. Compos. **33**, 138–146 (2012)
24. Katunin, A.: Domination of self-heating effect during fatigue of polymeric composites. Procedia Struct. Integrity **5**, 93–98 (2017)
25. Katunin, A.: A concept of thermographic method for non-destructive testing of polymeric composite structures using self-heating effect. Sensors **18**, 74 (2017)
26. Katunin, A., Wronkowicz, A.: Characterization of failure mechanisms of composite structures subjected to fatigue dominated by the self-heating effect. Compos. Struct. **180**, 1–8 (2017)
27. Katunin, A., Wronkowicz, A., Bilewicz, M., Wachla, D.: Criticality of self-heating in degradation processes of polymeric composites subjected to cyclic loading: A multiphysical approach. Arch. Civ. Mech. Eng. **17**, 806–815 (2017)
28. Katunin, A.: Evaluation of criticality of self-heating of polymer composites by estimating the heat dissipation rate. Mech. Compos. Mater. **54**, 53–60 (2018)
29. Katunin, A.: Criticality of the self-heating effect in polymers and polymer matrix composites during fatigue, and their application in non-destructive testing. Polymers **11**, 19 (2018)
30. Katunin, A., Wachla, D.: Analysis of defect detectability in polymeric composites using self-heating based vibrothermography. Compos. Struct. **201**, 760–765 (2018)
31. Katunin, A., Wachla, D.: Minimizing self-heating based fatigue degradation in polymeric composites by air cooling. Procedia Struct. Integrity **18**, 20–27 (2019)

32. Shou, Z., Chen, F., Yin, H.: Self-heating of a polymeric particulate composite under mechanical excitations. Mech. Mater. **117**, 116–125 (2018)
33. Di Maio, D., Magi, F.: Development of testing methods for endurance trials of composites components. J. Compos. Mater. **49**, 2977–2991 (2015)
34. Di Maio, D., Magi, F., Sever, I.A.: Damage monitoring of composite components under vibration fatigue using scanning laser doppler vibrometer. Exp. Mech. **58**, 499–514 (2018)
35. Magi, F., Di Maio, D., Sever, I.: Damage initiation and structural degradation through resonance vibration: application to composite laminates in fatigue. Compos. Sci. Technol. **132**, 47–56 (2016)
36. Magi, F., Di Maio, D., Sever, I.: Validation of initial crack propagation under vibration fatigue by finite element analysis. Int. J. Fatigue **104**, 183–194 (2017)
37. Voudouris, G., Di Maio, D., Sever, I.A.: Experimental fatigue behaviour of CFRP composites under vibration and thermal loading. Int. J. Fatigue **140**, 105791 (2020)
38. Smith, M.: ABAQUS/Standard User's Manual, Version 6.9. Dassault Systèmes Simulia Corp, Johnston (2009)
39. Benzeggagh, M.L., Kenane, M.: Measurement of mixed-mode delamination fracture toughness of unidirectional glass/epoxy composites with mixed-mode bending apparatus. Compos. Sci. Technol. **56**, 439–449 (1996)
40. Magi, F.: Vibration Fatigue Testing for Identification of Damage Initiation in Composites (2016)
41. Heidari-Rarani, M., Sayedain, M.: Finite element modeling strategies for 2d and 3d delamination propagation in composite DCB specimens using VCCT, CZM and XFEM approaches. Theor. Appl. Fract. Mech. **103**, 102246 (2019)
42. Masmeijer, T.: Vibration Fatigue Testing and Modeling for Identification of Damage Initiation and Propagation in Fiber Reinforced Plastics—University of Twente Student Theses (2021)
43. Heidari-Rarani, M., Shokrieh, M.M., Camanho, P.P.: Finite element modeling of mode i delamination growth in laminated DCB specimens with r-curve effects. Composites Part B: Engineering **45**, 897–903 (2013)